

# Limit on UHE neutrino flux from the Parkes lunar radio Cherenkov Experiment

C. W. James<sup>1\*</sup>, R. M. Crocker<sup>1</sup>, R. D. Ekers<sup>2</sup>, T. H. Hankins<sup>3</sup>, J. D. O’Sullivan<sup>2</sup>, R. J. Protheroe<sup>1</sup>

<sup>1</sup>Department of Physics, School of Chemistry & Physics, University of Adelaide, Adelaide SA 5000, Australia

<sup>2</sup>Australia Telescope National Facility, PO Box 76, Epping NSW 1710, Australia

<sup>3</sup>Physics Department, New Mexico Tech, Socorro, NM 87801, USA

24 December 2018

## ABSTRACT

The first search for ultra-high energy (UHE) neutrinos using a radio telescope was conducted by Hankins, Ekers & O’Sullivan (1996). This was a search for nanosecond duration radio Cherenkov pulses from electromagnetic cascades initiated by ultra-high energy (UHE) neutrino interactions in the lunar regolith, and was made using a broad-bandwidth receiver fitted to the Parkes radio telescope, Australia. At the time, no simulations were available to convert the null result into a neutrino flux limit. Since then, similar experiments at Goldstone, USA, and Kalyazin, Russia, have also recorded null results, and computer simulations have been used to model the experimental sensitivities of these two experiments and put useful limits on the UHE neutrino flux.

Proposed future experiments (Falcke, Gorham & Protheroe 2004) include the use of broad-bandwidth receivers, making the sensitivity achieved by the Parkes experiment highly relevant to the future prospects of this field. We have therefore calculated the effective aperture for the Parkes experiment and found that when pointing at the lunar limb, the effective aperture at all neutrino energies was superior to single-antenna, narrow-bandwidth experiments, and that the detection threshold was comparable to that of the double-antenna experiment at Goldstone. However, because only a small fraction of the observing time was spent pointing the limb, the Parkes experiment places only comparatively weak limits on the UHE neutrino flux. Future efforts should use multiple telescopes and broad-bandwidth receivers.

**Key words:** neutrinos – instrumentation: detectors – telescopes.

## 1 INTRODUCTION

The properties expected of ultra-high energy (UHE) neutrinos make them attractive targets for probing the high-energy universe. Unlike the highest energy photons and cosmic rays, a flux of neutrinos will not seriously suffer attenuation either at its source or during propagation. Being uncharged, the paths of neutrinos will remain unbent by galactic and intergalactic magnetic fields, so any detected neutrino should point back to its source. Additionally, any UHE neutrino flux should be very sensitive to the nature and evolution of the sources of the highest energy cosmic rays, providing a powerful discriminant between models of UHE cosmic ray production (Seckel & Stanev 2005).

The Lunar Cherenkov technique is a method by which UHE neutrinos may in principle be detected. Askaryan

(1962) described how a particle cascade in a dense medium produces coherent Cherenkov radiation. If the medium is transparent at radio frequencies, the radiation can escape and be detected remotely as a narrow pulse of a few nanoseconds duration, corresponding to decimetre and greater wavelengths. The lunar regolith (the outer layer of pulverised rock on the Moon’s surface) is such a radio-transparent medium, and as suggested by Dagkesamanskii & Zheleznykh (1989), observations of the Moon with ground-based radio-telescopes can be used to search for cascades produced by UHE neutrino interactions. This technique works in principle for both UHE cosmic rays and neutrinos, although formation-zone effects are expected to significantly reduce the cosmic ray signature (Gorham et al. 2001). At UHE the neutrino-nucleon cross section is such that neutrinos traversing the lunar diameter are severely attenuated. Together with subsequent shower and Cherenkov emission geometry, and refraction at the lu-

\* E-mail: clancy.james@adelaide.edu.au (CWJ)

nar surface, this causes GHz-regime Cherenkov signals to appear to originate almost entirely from the limb of the Moon.

The first attempt to use the lunar regolith in the search for UHE neutrinos was made at Parkes, Australia by Hankins, Ekers & O'Sullivan (1996). The 64 m Parkes radio telescope was used to observe the Moon for approximately 10.5 hours using a wide-bandwidth dual-polarisation receiver. No real events were recorded. Subsequently, two independent experiments utilising the technique also recorded null results, the first by Gorham et al. (2004) being the Goldstone Lunar Ultra-High Energy Neutrino Experiment (GLUE) that ran from 2001-2003 at NASA's Goldstone Deep Space Communications Complex, USA, and the second by Beresnyak et al. (2005) conducted from 2002 to 2004 at the Kalyazin Radio Astronomical Observatory, Russia. Importantly, both groups developed detailed simulations of the technique (see, respectively, Williams (2004) and Beresnyak (2004)). These were used to place limits on the UHE neutrino flux, with the published GLUE limit producing severe constraints on Z-burst UHE neutrino production models (Gorham et al. 2004).

The search for UHE neutrinos now encompasses a wide range of experiments, including the ANITA balloon experiment (Miočinović et al. 2005), low-frequency lunar observations with Westerbork and LOFAR (Scholten et al. 2006), and the Pierre Auger air-shower array (Billoir & Bigas 2006). Though no UHE neutrinos have so far been detected, limits placed on the UHE neutrino flux have already ruled out the more optimistic Z-burst models, and severely constrained the remainder (Barwick et al. 2006).

To ensure continuing competitiveness with these other efforts, future Lunar Cherenkov observations should aim to utilise 'next generation' radio-telescopes, in particular those designed as large arrays of smaller stations with broad-bandwidth receivers such as the planned SKA (Square Kilometre Array; Beck (2005)). In order to improve real-time discrimination of Cherenkov pulses from background noise and terrestrial RFI, the full capabilities offered of such instruments in nano-second pulse detection will have to be exploited. This will require the latest in signal processing technology. In parallel, sophisticated simulations should be used to optimise observation parameters such as frequency, beam pointing position, and bandwidth. A first step in this process is an analysis of the broad-bandwidth techniques developed at Parkes, the effectiveness of which we present here.

## 2 PARKES EXPERIMENT

The experiment at Parkes is described more fully by Hankins, Ekers & O'Sullivan (2001). Observations were on the nights of 16<sup>th</sup>, 17<sup>th</sup>, and 18<sup>th</sup> of January, 1995. At the time of observation, the significant limb-brightening effect had not been predicted and, unfortunately, only 2 hours out of the total 10.5 hours of observation time were spent pointing at the lunar limb. The remaining 8.5 hours, spent pointing at the centre, are not expected to contribute significantly to the sensitivity, as the entire limb was then outside the FWHM of the Parkes beam (13' at the central frequency of 1.5 GHz).

In the experiment, data from two polarisation channels

(LCP and RCP) for a 500-MHz band centred at 1.425 GHz were recorded. Triggering required a coincidence between two 100-MHz bandwidth sub-bands, centred at 1.325 and 1.525 GHz, extracted from either the LCP or RCP channel. The ionospheric delay between these sub-bands (estimated at 10 ns) was corrected for by artificially delaying the 1.525 GHz sub-band. Triggering occurred when the individual voltages in both the sub-bands simultaneously exceeded an  $8\sigma$  level (eight times the measured standard deviation of the oscilloscope voltage) for between 7.5 and 20 ns. This produced a trigger event approximately every two minutes.

The recorded data were processed to remove dispersion within each band. This also helped filter out terrestrial interference, which experiences no ionospheric delay (except any signals bounced off the Moon, which experience twice the dispersion). Pulses of coherent Cherenkov radiation were expected to be both 100% linearly polarised (and thus be received equally in both the LCP and RCP channels) and broad-band; these properties have since been experimentally verified (Saltzberg et al. 2001; Miočinović et al. 2006). The recorded data enabled candidate events to be tested for all these criteria, assuming a dispersion in the range of zero to twice that expected, a process which eliminated all of the  $\sim 700$  triggered events. Thus it was concluded that no Cherenkov pulse had been observed.

Only two 100MHz sub-bands could be used to form the trigger due to the limitations of signal processing technology in the mid '90s, where, ideally, the full 500MHz bandwidth with dual polarisation would have been used. This proved to be the limiting sensitivity as the remaining data (not used in triggering) proved more than adequate for discriminating RFI and thermal fluctuations. To demonstrate the usefulness of improved technology, it is useful to speculate about what the Parkes sensitivity might have been had the entirety of both data streams been de-dispersed in real-time and used to form a trigger. A proper estimate requires a knowledge of the precise effect of dedispersion on the amplitudes of RFI, which was responsible for the observed trigger rate and the setting of the  $8\sigma$  level. A conservative estimate, however, for the sensitivity can be obtained by assuming an identical trigger rate due to RFI, knowing that de-dispersion will act to reduce the amplitudes of the (undispersed) RFI signals. Therefore, we also present results for an otherwise identical Parkes experiment in which a signal strength of  $8\sigma$  in both of the full 500 MHz bands is required for detection. It should be possible to reduce this down to a  $\sim 6\sigma$  level on each channel in coincidence, which is the requirement to eliminate events from normally distributed thermal noise with 99.98% confidence at 1 GHz sampling over a 10.5 hr period.

## 3 SIMULATIONS

A Monte Carlo program was created to simulate the interactions of UHE neutrinos with the Moon, the production and propagation of coherent Cherenkov radiation, and the reception and triggering of the signal by the Parkes antenna. The program instantiates similar physics to the programs developed for the GLUE and the Kalyazin experiments. For UHE neutrinos at discrete energies a lunar impact parameter,  $r$ , was sampled from  $p(r) \propto r$  for  $0 < r < r_m$  where  $r_m$

is the lunar radius. The proportion of neutrinos detected by the simulated experiment was recorded and used to give an estimate of the detection probability per incident neutrino as a function of neutrino energy. To estimate the effective experimental aperture, the detection probability was multiplied by the physical lunar aperture ( $4\pi^2 r_m^2, \approx 1.21 \times 10^8 \text{ km}^2\text{-sr}$ ).

Both charged-current (CC) and neutral-current (NC) interactions of UHE neutrinos were modelled, with energy-dependent cross-sections taken from Gandhi et al. (1998). These interactions may initiate two kinds of showers. Electromagnetic showers consist entirely of  $\gamma$  and  $e^\pm$ , and are initiated only by the  $e^-/e^+$  produced in a  $\nu_e/\bar{\nu}_e$  CC-interaction, (bremsstrahlung photons from the  $\mu/\tau$  produced in  $\nu_\mu/\nu_\tau$  CC-interactions will be of insufficient energy to begin detectable cascades). Hadronic showers develop from both CC and NC interaction and consist of a hadronic core surrounded by an electromagnetic component (see Alvarez-Muñiz & Zas (2001) for a discussion of the relationship between Cherenkov radiation and shower phenomenology). The interaction inelasticity,  $y$  (fraction of neutrino energy given to hadronic showers), was sampled from the distributions used in Beresnyak (2004). In the case of  $\nu_e/\bar{\nu}_e$  CC interactions, where both electromagnetic and hadronic showers are present, only the shower with the strongest emission at a given angle to the shower axis was taken into account, because the relative phase between the two components is unknown. Neutrinos and anti-neutrinos were treated identically, as were  $\nu_\mu$  and  $\nu_\tau$ . One in three incident neutrinos was assumed to be a  $\nu_e/\bar{\nu}_e$  as we expect complete flavour mixing during oscillation over extragalactic distance scales Crocker et al. (2005).

The lunar density was modelled with five distinct density layers, with the densities of the inner four normalised so as to produce the correct lunar mass as in Williams (2004). The outer shell — nominally the regolith — was modelled with 10m depth, for consistency with both the simulations used by Gorham et al. (2004) and the results of radar and optical studies discussed by Shkuratov & Bondarenko (2001). A density of  $1.8 \text{ g/cm}^3$ , and refractive index  $n = 1.73$ , was used for consistency with the Cherenkov parameterisations of Alvarez-Muñiz et al. (2005).

Of these layers, only the regolith was treated as a suitable medium for the production of coherent Cherenkov radiation because of its known low attenuation at radio-frequencies. It appears reasonable to assume that the mega-regolith — a layer of ejecta blankets between the regolith and underlying bedrock in the lunar highlands, distinguished from the regolith as outlined by Short & Forman (1972), with an expected mean depth of  $\sim 2$  kms (Aggarwal & Oberbeck 1979) — may also exhibit low radio-attenuation properties. This region is treated by Scholten et al. (2006) as an extended regolith down to 500m depth. Detailed modelling of the production of Cherenkov radiation and radio-transmission through these surface layers of the Moon, including the depth dependence of their electromagnetic properties, is left to a future paper.

Neutrino interaction points were considered as point sources of Cherenkov radiation, with the Cherenkov cone axis being in the direction of the incoming neutrino. Previous simulations (Williams 2004; Beresnyak 2004) parameterised this radiation according to the results of

Alvarez-Muñiz & Zas (1997a) and Alvarez-Muñiz & Zas (2001) in ice and scaled these results to the regolith according to the prescription of Alvarez-Muñiz & Zas (1997b). Recently, Alvarez-Muñiz et al. (2005) obtained results for purely electromagnetic showers by simulating the regolith directly, using a refractive index of  $n = 1.73$ , density  $\rho = 1.8 \text{ g/cm}^3$ , radiation length  $X_0 = 22.59 \text{ g/cm}^2$ , and critical energy  $E_C = 40.0 \text{ MeV}$  (below which ionisation losses dominate bremsstrahlung). The value of the field strength at the Cherenkov angle was fitted as:

$$R |E_{\theta=\theta_C}(\nu)| = 8.45 \times 10^{-8} E_s \frac{\nu}{1 + \left(\frac{\nu}{\nu_R}\right)^\alpha} \text{ (V/MHz)} \quad (1)$$

for shower energy  $E_s$  (TeV), frequency  $\nu$  (GHz), and observation distance (i.e. Earth-Moon distance)  $R$  (m). The decoherence frequency  $\nu_R = 2.32 \text{ GHz}$ , and the scaling parameter  $\alpha = 1.32$ , have both been revised by Alvarez-Muñiz et al. (2005) from their former values of  $2.5 - 3.0 \text{ GHz}$  and  $1.44$  respectively. Notably, the normalisation of  $8.45 \times 10^{-8}$  is approximately 30% lower than the simple scaling relationships (Alvarez-Muñiz & Zas 1997b) would suggest, implying that the GLUE and Kalyazin apertures were over-estimated, particularly to lower neutrino energies (as discussed in Sec. 4).

Away from the Cherenkov angle, Alvarez-Muñiz et al. (2005) found the simple scaling relationships to be adequate to model the decoherence. However, these authors note the new parameterisation for radiation far from the Cherenkov angle is unreliable for shower energies at which the Landau-Pomeranchuk-Migdal (LPM) effect becomes important. This effect suppresses both the bremsstrahlung and pair-production cross-sections when the characteristic length of the interaction becomes comparable to distance between scattering centres (the atoms in the medium), and is important at particle energies above the LPM energy,  $E_{\text{LPM}}$ . For the regolith,  $E_{\text{LPM}} \approx 770 \text{ TeV}$ , which covers the entire UHE range, and therefore this new parameterisation for angular spread will be inappropriate for cascades initiated by UHE neutrinos. Simulations are currently in progress with showers in regolith for shower energies above the LPM energy. In the meantime, we have used Eqn. 1 to describe the peak field strength at the Cherenkov angle for electromagnetic showers, and take the angular dependence of purely electromagnetic showers from Alvarez-Muñiz & Zas (1997a), with the addition of the  $\sin \theta / \sin \theta_C$  term from Alvarez-Muñiz et al. (2005). The characteristic width  $\Delta\theta$  we assumed to scale with  $\rho/X_0/\sqrt{n^2 - 1}$  ( $X_0$  the radiation length;  $X_0 = 22.59 \text{ g/cm}^2$  here). Thus we assume the Cherenkov cone to be approximately 3.4 times as wide in the regolith as in ice.

The Cherenkov radiation from hadronic showers is derived almost entirely from electromagnetic sub-showers resulting from  $\pi^0$ -decay into  $\gamma$ -rays. Because of the similar phenomenology, the peak pulse strength for hadronic showers can be derived by multiplying the purely electromagnetic result, Eqn. 1, by an energy-dependent correction function, which is approximately the fraction of energy going into electromagnetic sub-showers (Alvarez-Muñiz & Zas 1998). Originally calculated for cascades in ice, the medium-dependence of this function has yet to be investigated, and so to calculate the peak pulse strength for hadronic showers we used it unmodified with the electromagnetic result for the re-

golith described above. The cone-width for hadronic showers was also taken from Alvarez-Muñiz & Zas (1998), extrapolated above 10 EeV as per Williams (2004), and scaled to the regolith as with the electromagnetic shower width.

In the Monte Carlo code the Cherenkov emission is represented as bundles of “rays”, each ray having associated with it a direction, solid angle, field strength and polarisation. Ray-tracing was used to propagate the radiation to Earth, at distance  $R = 3.844 \times 10^8$  m. Modelled effects included the electric-field attenuation length  $\ell$  in the regolith ( $\ell = 18$  m at 1 GHz;  $\ell \propto 1/f$ ), refraction at the lunar surface using the Fresnel transmission coefficients for each component of the polarisation, and the solid-angle-stretching factor applicable to a point source.

Surface roughness was simulated by randomly deviating the local surface normal from the perpendicular. The deviation angle (the adirectional slope) was calculated by generating the slope tangents (unidirectional slopes) in orthogonal directions, which are gaussian-distributed with mean 0 and variance  $\arctan^2(6^\circ)$ , where  $\arctan(6^\circ)$  is the RMS surface roughness used in Beresnyak (2004). This accounted for large-scale surface roughness, such as hill-sides and crater walls, with dimensions larger than the shower size. The effects of intermediate-scale surface roughness, on scales between the wavelength and shower size, is not currently understood sufficiently to be included.

As with previous simulations, dispersion in the ionosphere was assumed negligible within each 100 MHz sub-band, and the height of the pulse was calculated by summing the contributions across the bandwidth. The signal was assumed to retain its 100% polarisation, and thus be received with 50% power efficiency by each of the circularly-polarised receivers. As lunar thermal emission was the dominant source of noise, the ratio of total signal (true UHE neutrino signature plus a random noise component) to mean thermal noise is preserved by the electronics; hence, detection could be determined without the need to simulate the response of the Parkes receiver system. This simplification is justified by the low background noise recorded when pointing off the Moon.

## 4 RESULTS

The simulation was run for energies in the range  $10^{19}$ – $10^{24}$  eV. The calculated aperture for both centre-pointing and limb-pointing configurations of the Parkes experiment is plotted in Fig. 1, together with the simulation results for the GLUE experiment. No aperture has been published for the Kalyazin experiment which had a threshold of 13,500 Jy. However, the simulation results of Beresnyak (2004), in which an otherwise identical experiment with an assumed threshold of 3,000 Jy is modelled, have been included, together with estimates for the improved Parkes experiment described in Sec. 2.

In comparing the apertures, note that the parameters we used to simulate the Parkes experiment, such as depth of regolith, amplitude of Cherenkov radiation, and mean surface roughness, are at least as pessimistic as those of either Williams (2004) or Beresnyak (2004). Furthermore, perhaps because of parameter differences, these two previous simulations produce apertures which differ by an order

of magnitude at  $10^{23}$  eV, as first noted in Beresnyak et al. (2005). This is surprising, firstly because of the similarity of the modelled experiments, as opposed to the actual experiments, and secondly because the greater difference is at high energies where naively one would expect the results to be less sensitive to differences in the modelling.

In more detail, consider lowering the simulated signal strength by 10%. This will produce a much lower effective aperture to neutrinos near the threshold energy for neutrino detection, where all simulated detections are marginal. However, a neutrino of 100 times this energy will produce a coherent Cherenkov signal with  $100^2$  times the power, so that simulated detections include only a very small fraction of marginal events. Hence, the effect of lowering the modelled signal strength will be relatively smaller for higher energy neutrino events. This is why the calculated apertures have a stronger energy dependence at low neutrino energies: the Parkes limb aperture at  $10^{22}$  eV is 13.8 times that at  $10^{21}$  eV, but the aperture to  $10^{24}$  eV neutrinos is only 3.9 times that at  $10^{23}$  eV (noting that a factor of 2.3 per decade arises naturally from the increasing neutrino cross-section).

Putting these concerns aside, Fig. 1 clearly demonstrates the benefits of the wide-bandwidth system used at Parkes. The effective energy threshold of  $\sim 3 \times 10^{20}$  eV for the limb-pointing configuration is similar to that achieved by both GLUE (which utilised two antennae) and Kalyazin (basing this on the simulation of Beresnyak (2004), which assumed a sensitivity of 3,000 Jy instead of the eventual 13,500 Jy). Above threshold energies, the Parkes aperture consistently lies below that from GLUE and above that of Kalyazin, a comparison which could only be improved by the use of identical simulation methods.

An unambiguous result is the desirability of pointing at the limb. Compared to the limb-pointing, the centre-pointing configuration of the Parkes experiment exhibits an order of magnitude higher effective energy threshold ( $\sim 4 \times 10^{21}$  vs  $\sim 4 \times 10^{20}$  eV), and even at  $10^{23}$  eV the effective aperture is less than half that at the limb. This effect was partially off-set in the GLUE experiment by defocussing the 70m dish when not pointing at the limb, which accounts for the smaller difference in apertures between configurations at  $10^{22}$  eV. For experiments utilising lower frequencies and smaller dishes, in which the FWHM of the beam is comparable to, or greater than, the apparent size of the Moon, the effect will likely be negligible.

The importance of developing signal processing techniques is shown by the lower detection threshold and greater aperture which would have resulted if the experiment at Parkes had been able to utilise all available data in forming a trigger. As expected, the difference is most pronounced at low energies, with the increased sensitivity effected by the use of a wider bandwidth in triggering shifting the effective aperture to the left. Methods to increase the aperture at higher energies include the use of multiple beams to cover the entire limb, and/or smaller antennas to cover the entire Moon with a single beam. These will be discussed in a future paper.

The effect of the lower observation frequency at Parkes is also evident. As discussed in detail by Scholten et al. (2006), Cherenkov radiation escapes the Moon more readily at low frequencies, and the increase in beam size also allows more of the Moon to be observed. The disadvantage is a

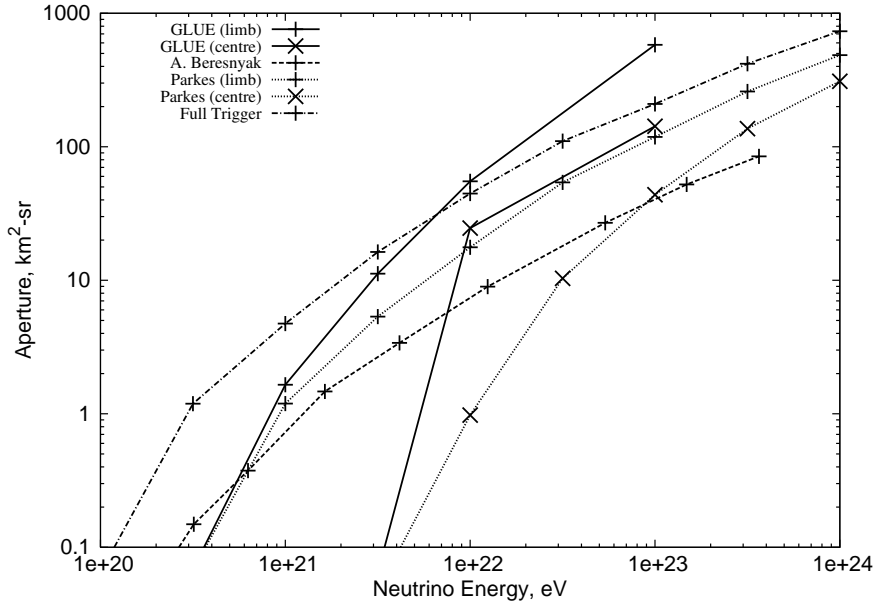


**Figure 1.** Effective apertures ( $\text{km}^2\text{-sr}$ ) as a function of neutrino energy (eV) of Lunar radio-Cherenkov experiments: GLUE (solid curve, taken from Williams (2004)), Kalyazin (dashed, from Beresnyak (2004)), and Parkes (dotted; our calculations). The symbols indicate pointing position (+ limb;  $\times$  centre). Also plotted (dot-dashed) are our estimates for Parkes utilising all available data in forming a trigger. As discussed in the text, the plotted prediction for Kalyazin used an optimistic detection threshold, and the true sensitivity, particularly for the lower neutrino energies, will have been less.

lower sensitivity because the Cherenkov signal is weaker at low frequencies, and the lower noise power per beam solid angle from lunar thermal emission is mostly offset by the increased beam size. The result is a steeper increase in aperture with energy as is evident from Fig. 1 – at  $10^{21}$  eV, the Parkes aperture is 1.5 times that of Beresnyak’s result for Kalyazin, whereas at  $10^{23}$  eV it is three times larger.

The limit on the UHE neutrino flux we derive for the Parkes experiment is plotted in Fig. 2. The contribution from the 8.5 hours spent pointing at the lunar centre is negligible and, with only 2 hours of useful limb observations, the UHE neutrino flux limit from the Parkes experiment is much weaker than that from either the Kalyazin experiment (31.3 hrs (Beresnyak et al. 2005)) or Goldstone experiments (73.45 hrs limb, 40 hrs half-limb (Williams 2004)).

## 5 CONCLUSIONS

We have calculated the effective aperture of the Parkes experiment, and found that in the limb-pointing configuration it was a competitive experiment as the exposure to UHE neutrinos per hour of observation time was greater than the single-dish experiment at Kalyazin, and it achieved an effective neutrino detection energy threshold equal to that of the two-telescope experiment at Goldstone. Unfortunately, the centre-pointing configuration, where most of the observation time was spent, had negligible sensitivity at all but the highest energies. The resulting limits on the UHE neutrino flux from the present Parkes experiment are therefore not competitive with those from either GLUE or Kalyazin.

Clearly, using the broad-band techniques at Parkes with modern signal processing technology would greatly improve the sensitivity of future searches for Lunar Cherenkov emis-

sion, even without improved RFI discrimination. This could be provided by utilising multiple antennas, as in GLUE, or by using intelligent hardware which incorporates the discriminants currently used in off-line processing into a real-time trigger. Future experiments should aim to use both. The next generation of radio-telescopes, such as LOFAR and the SKA, both of which will use large arrays of antennae linked by high speed connections, will prove ideal instruments for the UHE neutrino search, and may give the best chance to detect these elusive particles.

## ACKNOWLEDGMENTS

This research was supported under the Australian Research Council’s Discovery funding scheme (project number DP0559991). Professor R. D. Ekers is the recipient of an Australian Research Council Federation Fellowship (project number FF0345330). C. W. James thanks Dr. T. Kneiske for assistance with simulation development, and J. Alvarez-Muñiz for discussions on the scaling of coherent Cherenkov radiation.

## REFERENCES

- Aggarwal H. R., Oberbeck V. R., 1979, Proc 10<sup>th</sup> Lunar Planet. Sci. Conf., 2689
- Alvarez-Muñiz J., Zas E., 1997, Phys. Lett. B, 411, 218
- Alvarez-Muñiz J. & Zas E., 1997, Proceedings of the XXV International Cosmic Ray Conference, Durban, South Africa, 7, 309
- Alvarez-Muñiz J., Zas E., 1998, Phys. Lett. B, 434, 396
- Alvarez-Muñiz J., Zas, E., 2001, astro-ph/0103369
- Alvarez-Muñiz et al., 2005, astro-ph/0512337 v1

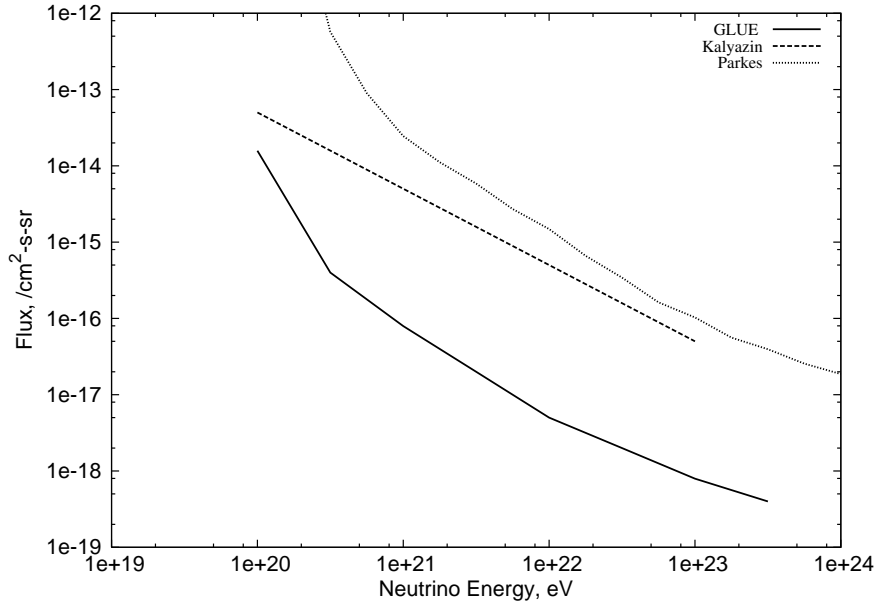


**Figure 2.** UHE neutrino flux limits derived from lunar Cherenkov observations. The limit from Parkes (dotted) has been calculated as in Gorham et al. (2004) for GLUE (solid, from Williams (2004)), by inverting the product of effective aperture and observation time, and multiplying by 2.3 (for 90% confidence under Poisson statistics). The limits from the Kalyazin experiment (dashed) are taken from Beresnyak et al. (2005), and were expressed as a 95% limit on an  $E^{-2}$  spectrum between  $10^{20}$  eV and  $10^{23}$  eV.

Askary'an G. A., 1962, Sov. Phys. JETP, 14, 441  
 Barwick S. *et al.*, 2006, Phys. Rev. Lett., 96, 171101  
 Beck, R. 2005, Astronomische Nachrichten, 326, 608  
 Beresnyak A. R., 2004, astro-ph/0310295 v2  
 Beresnyak A. R. *et al.*, 2005, Astronomy Reports, 49, 127  
 Billoir P., Bigas O. B., 2006, The Pierre Auger Observatory and neutrinos (Subm. to Neutrino Oscillation Workshop NOW 2006, September 9 - 16, 2006, Conca Specchiulla, Otranto, Italy)  
 Crocker, R. M., Melia, F., & Volkas, R. R. 2005, ApJ Lett. 622, L37  
 Dagkesamanskii R. D., Zheleznykh I. M., 1989, Sov. Phys. JETP Let., 50, 233  
 Falcke H., Gorham P., Protheroe R. J., 2004, New Astron. Rev., 48, 1487  
 Gandhi R. *et al.*, 1998, Phys. Rev. D, 58, 093009  
 Gorham P. W. *et al.*, 2001, in Saltzberg D., and Gorham P. W., eds, Radio Detection of High Energy Particles — RADHEP 2000, AIP Conf. Proc. No. 579. AIP, New York, p177  
 Gorham P. W. *et al.*, 2004, Phys. Rev. Lett., 93, 041101  
 Hankins T. H., Ekers R. D., O'Sullivan J. D., 1996, MNRAS, 283, 1027  
 Hankins T. H., Ekers R. D., O'Sullivan J. D., 2001, in Saltzberg D., and Gorham P. W., eds, Radio Detection of High Energy Particles — RADHEP 2000, AIP Conf. Proc. No. 579. AIP, New York, p168  
 Miočinović P. *et al.*, 2005, astro-ph/0503304 v1  
 Miočinović P. *et al.*, 2006, Phys. Rev. D, 64, 043002  
 Saltzberg D. *et al.*, 2001, Phys. Rev. Lett., 86, 2802  
 Scholten O. *et al.*, 2006, Astropart. Phys., 26, 219  
 Shkuratov Y. G., Bondarenko N. V., 2001, Icarus, 149, 329  
 Short N. M., Forman M. L., 1972, Modern Geology, 3, 69  
 Seckel D., Stanev T., 2005, Phys. Rev. Lett. D, 95, 041101  
 Williams D. R., 2004, The Askar'yan Effect and Detection

of Extremely High Energy Neutrinos in the Lunar Regolith and Salt, Dissertation, University of California

This paper has been typeset from a *TeX*/ *LATeX* file prepared by the author.